On the Usefulness of Outer-Loop Power Control With Successive Interference Cancellation

R. Michael Buehrer, *Member, IEEE*, and Rahul Mahajan, *Student Member, IEEE*

***Abstract*—It is well known that multiuser detection can obtain significant performance advantages over the conventional matched filter receiver in code division multiple access systems. Further, since optimal multiuser detection is exponentially complex, the majority of research has focused on suboptimal approaches such as successive interference cancellation (SIC). SIC has been shown to require a geometric distribution of received powers to achieve equal performance for all received signals. In this paper we propose a power control scheme for SIC to achieve this profile (or the profile corresponding to any desired and achievable set of error rates) based on frame-error rate (FER) or bit-error rate (BER). Specifically, we derive the relationship between received power and BER for linear SIC and show that for unlimited mobile powers, a deterministic distributed BER-based outer-loop power control will drive the received powers to the optimal power profile. The convergence of the deterministic BER-based algorithm is examined in the absence of inner loop power control errors. The simulated performance of a stochastic version of this algorithm is examined using instantaneous FER measurements. The stochastic algorithm is shown to provide unbiased estimates of the true power updates and converge to the optimal power vector provided the mobiles have unlimited power. Further, we consider power limits for specific mobiles and find that individual mobile limits do not affect the performance of other signals. Further, we examine the impact of system loading, multiple FER targets, error correction, and inner loop power control error on the performance of the algorithm.**

***Index Terms*—Code-division multiple access (CDMA), multiuser detection, power control, spread spectrum, successive interference cancellation (SIC).**

I. INTRODUCTION

SINCE the advent of code-division multiple access (CDMA) in commercial wireless systems, the area of multiuser detection has been an area of intense research [1]–[3]. One form of suboptimal multiuser detection, successive interference cancellation, or SIC, has received significant attention [4]–[9]. One difficulty in the implementation of SIC is that for equal received signal strengths, the bit-error rate (BER) performance will vary significantly. Power control in current CDMA systems is designed to guarantee approximately equal received power for all signals using a combination of inner loop and outer-loop power control. To obtain equal BER for all signals with SIC, the received power profile must vary geometrically according to the cancellation order [4], [7], [9], [10]. Creating power control tables which have unequal signal-to-interference ratio (SIR) thresholds to maintain such received power levels using inner loop power control could be problematic. In this paper, we show that frame-error rate (FER)-based (or equivalently BER-based) outer-loop power control will provide sufficient control for SIC without using different power control tables and without causing a degradation in SIC performance. Further, using outer-loop control to guarantee BER performance with SIC simply requires a coarse knowledge of the power limits of the mobile. That is, we must use some knowledge of the relative shadow fading and path loss experienced by each mobile to determine the cancellation order. This information is available from the output of the receiver's acquisition and searcher circuits or via mobile measurements taken for mobile-assisted handoff decisions. We show that, for the cases examined, when the power limits are known incorrectly, only the performance of the signal in question is affected, and catastrophic system failure does not occur. In the next section, we briefly discuss previous work considering power control with multiuser detection in CDMA systems as well as the proposed power control method. In Section III we describe the system model assumed and describe successive interference cancellation. The convergence of a deterministic BER-based power control for SIC receivers is analyzed in Section IV and a brief discussion of the stochastic version of this algorithm is given in Section V. Simulation results are presented in Section VI which show the behavior of the average received power and frame error rate when using FER-based outer-loop power control with SIC under various conditions including different loading conditions, multiple FER targets, with and without error correction coding and imperfect inner loop power control.

II. POWER CONTROL IN CDMA

Power control is an extremely important part of current CDMA systems. If multiuser detection is to play a part in commercial CDMA, its interaction with power control must be well understood. Compared to the massive amount of work done on multiuser detection, to date relatively little work has been done on the interaction between power control and multiuser detection [11]–[16]. The combination of power control with the linear minimum mean-square error (MMSE) receiver was considered in [11]–[15] while [16] considered power control with the linear decorrelator.

Further, the impact of power control with SIC on system interference levels was analyzed in [9] although the method of power control was not discussed. All of the approaches considered signal-to-interference-plus-noise ratio (SINR)-based measurements at the base station which were used to determine an

Paper approved by S. L. Miller, the Editor for Spread Spectrum of the IEEE Communications Society. Manuscript received August 1, 2001; revised November 19, 2002 and June 19, 2003. This paper was presented in part at the Vehicular Technology Conference, Vancouver, BC, Canada, Fall 2002.

The authors are with the Mobile and Portable Radio Research Group (MPRG), Virginia Polytechnic Institute and State University, Blacksburg, VA 24061 USA (e-mail: buehrer@vt.edu).

Digital Object Identifier 10.1109/TCOMM.2003.820756

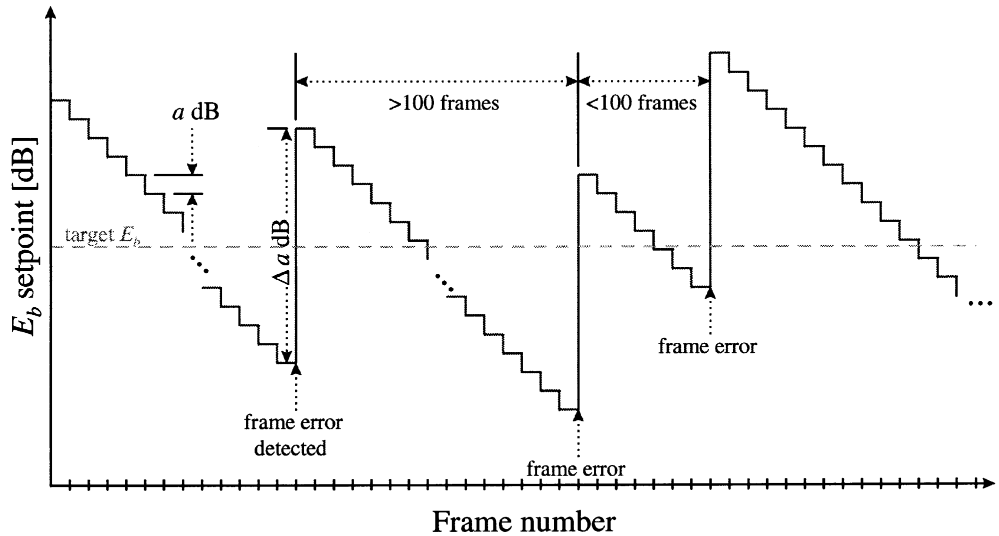

Fig. 1. Illustration of FER-based E_b/I_o set-point control.

optimal power setting for each mobile. This information was then communicated back to the mobile for power adjustment. Essentially, these methods can be considered "outer loop" techniques since they are aimed at adjusting long-term power to provide an optimal received power distribution between users. This is as opposed to "inner loop" control which makes fine adjustments to counter Rayleigh fading. None of the studies mentioned were concerned with the effects of inner loop control and we will likewise ignore this effect during most of this examination. We will briefly examine the impact of inner loop power control error via simulation in Section VI.

In contrast to these techniques, we propose here an FER-based approach for reverse link power control to be used in conjunction with SIC as is commonly done with matched filter receivers. Traditional reverse link power control is accomplished by transmitting power control bits on the forward link to the mobile unit on which it bases its decisions to increase or decrease transmit power. Simply viewed, each power control group (PCG)[1] the base station receiver estimates E_b/I_o and compares this estimate with an internally saved threshold which is known as the E_b/I_o set-point. If the estimate of E_b/I_o is less than the E_b/I_o set-point, the power control bit is set to zero during the next PCG transmitted on the downlink. Otherwise, it is set to one. The mobile station interprets a zero as a request for more transmit energy, and a one as a request for less. This type of E_b/I_o-based power control is often called "fast power control" since it operates at a rate of up to 800 Hz (in *cdma2000*) and is intended to combat short-term multipath fading.

What we have described thus far is only the "inner loop" portion of E_b/I_o-based power control. What happens with the E_b/I_o set-point is referred to as the "outer loop." In FER-based outer-loop power control, after every frame the base station receiver determines whether it made an error in decoding or not via cyclic redundancy check (CRC) or some other method. If the frame is in error, the base station may raise its set-point by some value. If the frame is not in error, the base station may lower its set point by some (usually smaller) value. In this manner, a target FER may be maintained. If, for example, a $y\%$ FER is desired, the receiver should raise its set-point by Δ dB when it records an error. The down step a is then given by

$$a = \Delta \cdot \frac{y}{100 - y} \text{ dB}. \tag{1}$$

This is depicted in Fig. 1. Over time, this raising and lowering of the set point is intended to result in the desired target FER. Maintenance of a desired FER is crucial to the capacity of virtually any CDMA system since one mobile station's signal is interference for the rest. This interference ultimately limits system capacity. We will show that this power control method can be used with SIC in this work.

III. System Model and Analysis

We consider a CDMA system with K active transmitters communicating with a common base station. For ease of analysis we consider a single cell. The received signal at the base station can be expressed in complex baseband notation as

$$r(t) = \sum_{k=1}^{K} \sqrt{P_k(t)} b_k(t - \tau_k) a_k(t - \tau_k) e^{j\phi_k(t)} + n(t) \tag{2}$$

where P_k is the received power from transmitter k, $b_k(t)$ and $a_k(t)$ are the data and random spreading waveforms of the kth signal, respectively, τ_k and ϕ_k are the relative delays and phases of each signal with respect to an arbitrary reference, and $n(t)$ is a complex Gaussian random process with variance σ_n^2 and represents thermal noise. The combination of $\sqrt{P_k(t)}e^{j\phi_k(t)}$ is the complex distortion caused by the wireless channel. For the purpose of this investigation we assume that inner loop power control is perfect or that fading is sufficiently slow such that P_k and ϕ_k are constant over the observation interval (i.e., a frame). Thus, the effect of fading due to inner loop power control error is not explicitly considered.[2]

[1]A power control group or PCG is equivalent to 1.25 ms in IS-95 and *cdma2000*.

[2]We briefly ease this restriction in Section VI.

A SIC receiver attempts to detect signals in succession by cancelling each signal from the aggregate received signal after detection [4]. We represent the signal used to detect data from signal k as

$$r^{(k)}(t) = r(t) - \sum_{i=1}^{k-1} \hat{s}_i(t-\tau_i) \tag{3}$$

where $s_i(t) = \sqrt{P_i} b_i(t) a_i(t) e^{j\phi_i}$ and $\hat{s}_i(t)$ are the received signal and the estimate of the received signal from mobile i. In this work we consider a *linear* receiver in which the estimated signal is a linear transform of the received signal. Specifically, we estimate the received signal as

$$\hat{s}_k(t) = \sum_{m=-\infty}^{\infty} z_{k,m} p_T(t-mT) a_k(t) \tag{4}$$

where $p_T(t)$ is a unit pulse defined on $[0,T)$, $z_{i,m}$ is the projection of the received signal onto the spreading code of signal i after cancellation of signal $i-1$ during the mth symbol interval, i.e.,

$$z_{k,m} = \frac{1}{T} \int_{(m-1)T+\tau_k}^{mT+\tau_k} r^{(k)}(t) a_k^*(t-\tau_k) dt. \tag{5}$$

T is the symbol duration and * represents the complex conjugate.

To examine the performance of the successive cancellation receiver described above, we will examine the decision statistic more closely. Using (3) in (5) we rewrite $z_{k,m}$ as

$$\begin{aligned} z_{k,m} &= \frac{1}{T}\left[\int_{(m-1)T+\tau_k}^{mT+\tau_k} \left(\sum_{i=1}^{K} s_i(t-\tau_i) \right) a_k^*(t-\tau_k) dt \right. \\ &\quad \left. - \int_{(m-1)T+\tau_k}^{mT+\tau_k} \left(\sum_{i=1}^{k-1} \hat{s}_i(t-\tau_i) \right) a_k^*(t-\tau_k) dt \right] + N_{k,m} \\ &= \sqrt{P_k} b_{k,m} e^{j\phi_k} + \sum_{i=1}^{k-1} \tilde{I}_{k,i,m} + \sum_{i=k+1}^{K} I_{k,i,m} + N_{k,m} \end{aligned} \tag{6}$$

where $N_{k,m} = (1/T)\int_{(m-1)T+\tau_k}^{mT+\tau_k} n(t) a_k^*(t-\tau_k) dt$, $I_{k,i,m}$ is the cross correlation between signal k and signal i during signal k's mth bit interval, and $\tilde{I}_{k,i,m}$ is the residual cross correlation between signals after cancellation.[3] Now, if a Gaussian assumption is made on the decision statistic as is commonly done in CDMA system analysis[4] we are interested in the second-order statistics of $z_{k,m}$ [17]. Namely, we define the SINR for signal k as

$$\Gamma_k = \frac{\mathrm{E}^2\left\{\Re\left[z_{k,m}\gamma_k^*\right] | b_{k,m}\right\}}{\mathrm{var}\left\{\Re\left[z_{k,m}\gamma_k^*\right] | b_{k,m}\right\}} \tag{7}$$

[3]The above formulation neglects the effects of uncancelled future bits. This is justifiable when either: 1) the system is synchronous; 2) the relative delays of all signals satisfy $\{\tau_k\} \ll T$; or 3) cancellation is done on blocks of simultaneous bits.

[4]This assumption is commonly made in the case of successive cancellation where it may be less justified than in the case of simple matched filtering [5], [6].

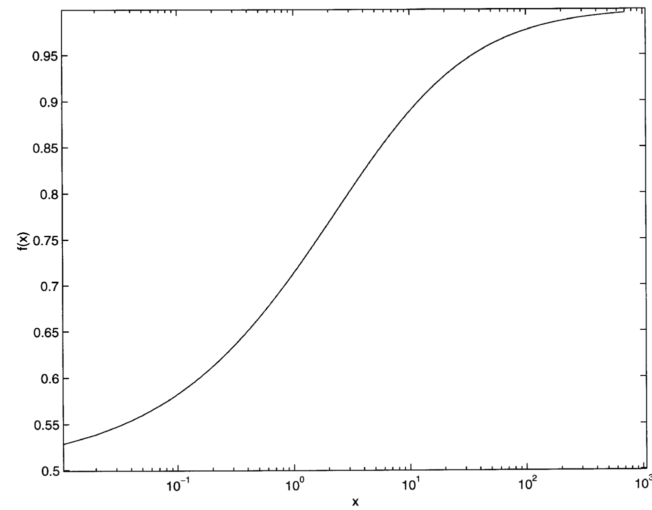

Fig. 2. Convergence of (21).

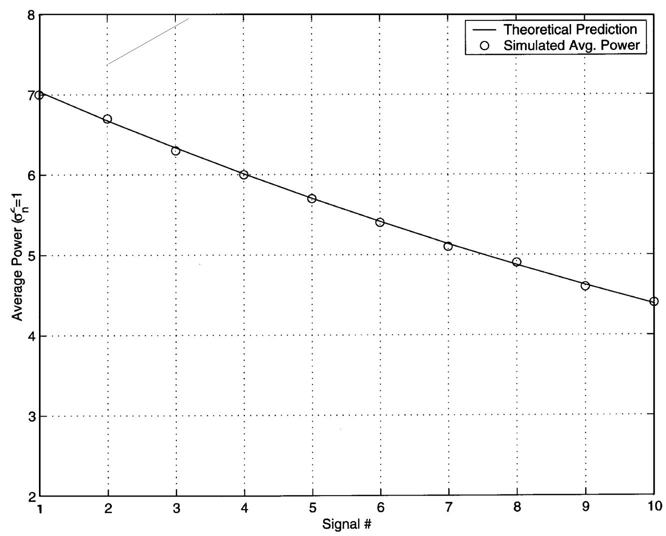

Fig. 3. Simulated and theoretical normalized ($\sigma_n^2 = 1$) received powers for 12% target FER using stochastic FER-based outer-loop power control with SIC (perfect inner loop power control is assumed, $N = 64$, $K = 10$).

where $\gamma_k = \sqrt{P_k} e^{j\phi_k}$ is obtained from the channel estimation process (e.g. from the pilot channel) and we ignore the impact of imperfect channel estimation. From [10] we can write the SINR of signal $k(\Gamma_k)$ as

$$\Gamma_k = \left\{ \left[\frac{\sigma^2}{P_k} + \frac{\varrho}{N} \sum_{i=2}^{K} \frac{P_i}{P_k} \right] \left(1 + \frac{\varrho}{N}\right)^{k-1} - \frac{\varrho}{N} \sum_{i=2}^{k} \left(1+\frac{\varrho}{N}\right)^{k-i} \frac{P_i}{P_k} \right\}^{-1} \tag{8}$$

where for rectangular chips

$$\varrho = \begin{cases} 1, & \text{synchronous, zero phase} \\ \frac{1}{2}, & \text{synchronous, random phase} \\ \frac{2}{3}, & \text{asynchronous, zero phase} \\ \frac{1}{3}, & \text{asynchronous, random phase.} \end{cases} \tag{9}$$

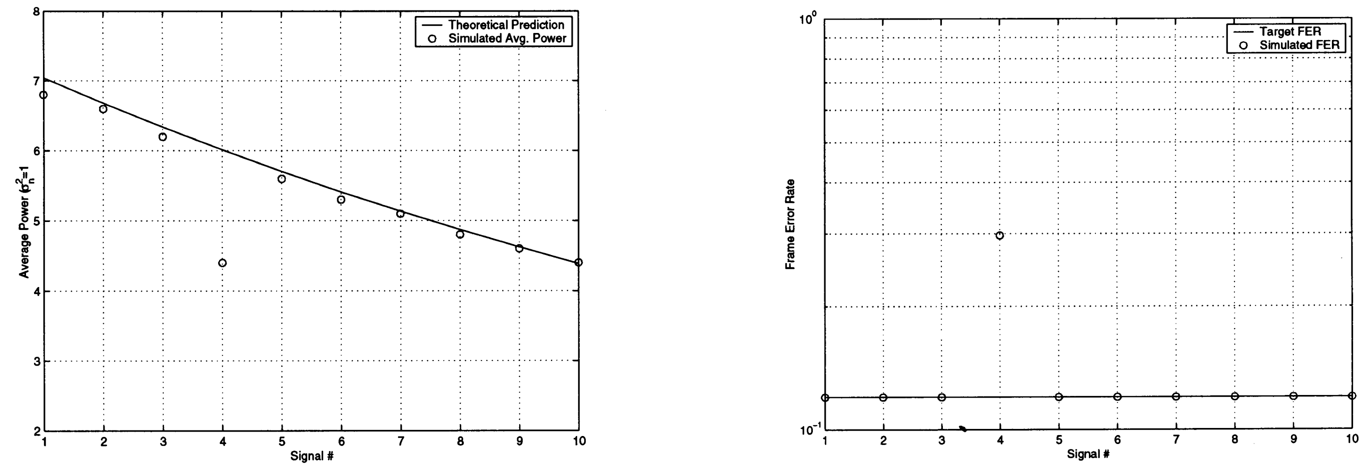

(a) (b)

Fig. 4. (a) Simulated and theoretical normalized ($\sigma_n^2 = 1$) received powers and (b) resulting FER for 12% target FER using FER-based outer-loop power control with SIC (perfect inner loop power control is assumed, $N = 64$, $K = 10$, signal 4 has received power limit of 4.4).

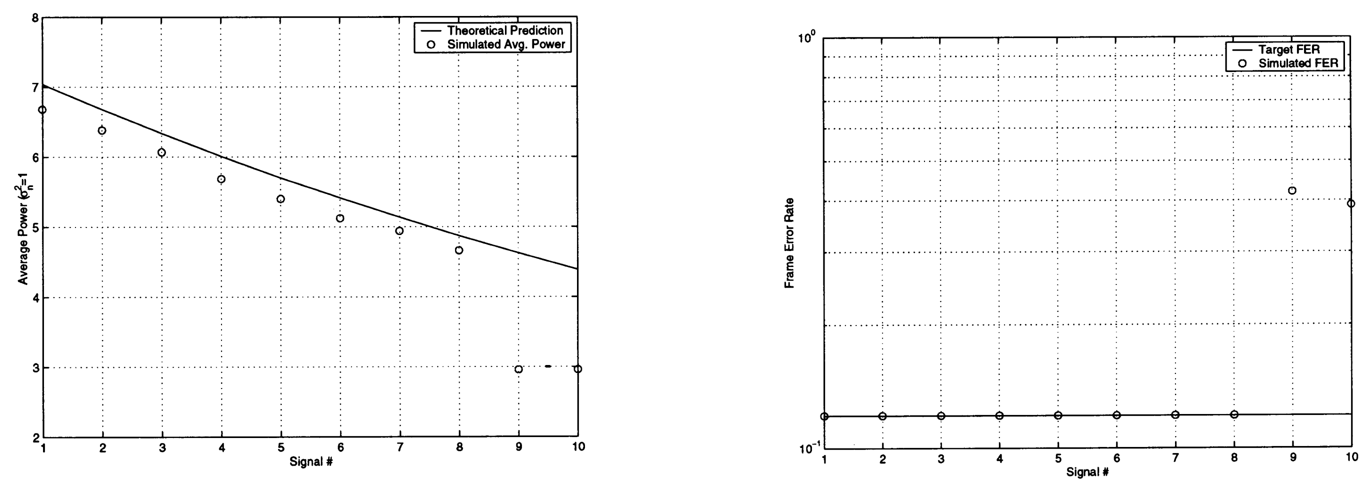

(a) (b)

Fig. 5. (a) Simulated and theoretical normalized ($\sigma_n^2 = 1$) received powers and (b) resulting FER for 12% target FER using FER-based outer-loop power control with SIC (perfect inner loop power control is assumed, $N = 64$, $K = 10$, signals 9 and 10 have received power limits of 3.0).

Further, it is shown in [10] that the given receiver can provide equal SINR (i.e., $\Gamma_k = \Gamma \forall k$) and, thus, equal BER if the following power profile is used:

$$\boxed{\mathbf{p}_{\text{opt}} = \left(\tfrac{1}{\Gamma}\mathbf{I} - \tfrac{\varrho}{N}\mathbf{X}\right)^{-1}\beta\sigma^2} \tag{10}$$

where $\mathbf{p} = [P_1, P_2, \ldots P_k]^T$, $\mathbf{I}$ is a $K \times K$ identity matrix, $\boldsymbol{\beta}$ is a $K \times 1$ vector with $(1 + (\varrho/N))^{i-1}$ as the ith element, $\mathbf{X}$ is a $K \times K$ matrix with $\mathbf{x}_i^T$ as the ith row and $\mathbf{x}_k$ is a $K \times 1$ vector defined as

$$x_{k,m} = \begin{cases} 0, & m = 1 \\ \left(1 + \frac{\varrho}{N}\right)^{k-1} - \left(1 + \frac{\varrho}{N}\right)^{k-m}, & m \le k \\ \left(1 + \frac{\varrho}{N}\right)^{k-1}, & m > k. \end{cases} \tag{11}$$

The optimal power profile is shown for $K = 10$, $N = 31$, $\varrho = 1/2$, $\Gamma = 6$ dB, and $\sigma_n = 1$ (curve is labeled "Theoretical Prediction"). Note that this profile makes no assumptions about perfect cancellation. We can see that each signal requires a different received power to obtain equal BER based on cancellation order. User 1 requires the least power since it is cancelled last (i.e., it receives the most benefit from cancellation). User K requires the most power since it is cancelled first and benefits the least from cancellation.

Equation (10) applies to the case of equal BER requirements (e.g., voice networks). In the case where there are different BER requirements, the desired power profile is

$$\boxed{\mathbf{p}_{\text{opt}} = \left(\mathbf{Q}^{-1} - \tfrac{\varrho}{N}\mathbf{X}\right)^{-1}\beta\sigma^2} \tag{12}$$

where $\mathbf{Q} = \text{diag}\{\boldsymbol{\Gamma}\}$, $\text{diag}\{\mathbf{x}\}$ is a diagonal matrix with $\mathbf{x}$ on the diagonal and $\boldsymbol{\Gamma}$ is the vector of SINR values needed to obtain the desired set of error rates. Using a Gaussian approximation, the BER is $Q(\sqrt{2\boldsymbol{\Gamma}})$ where the output of $Q(\boldsymbol{x})$ is a vector with each element being the standard Q-function operating on each element of $\boldsymbol{x}$.

Thus, we could use the above values[5] to directly set the E_b/I_o set-point for the inner power control loop in order to provide

[5]The exact levels would have to be adjusted for the number of Rake fingers and would be dependent on the measurements being used for power control at the base station.

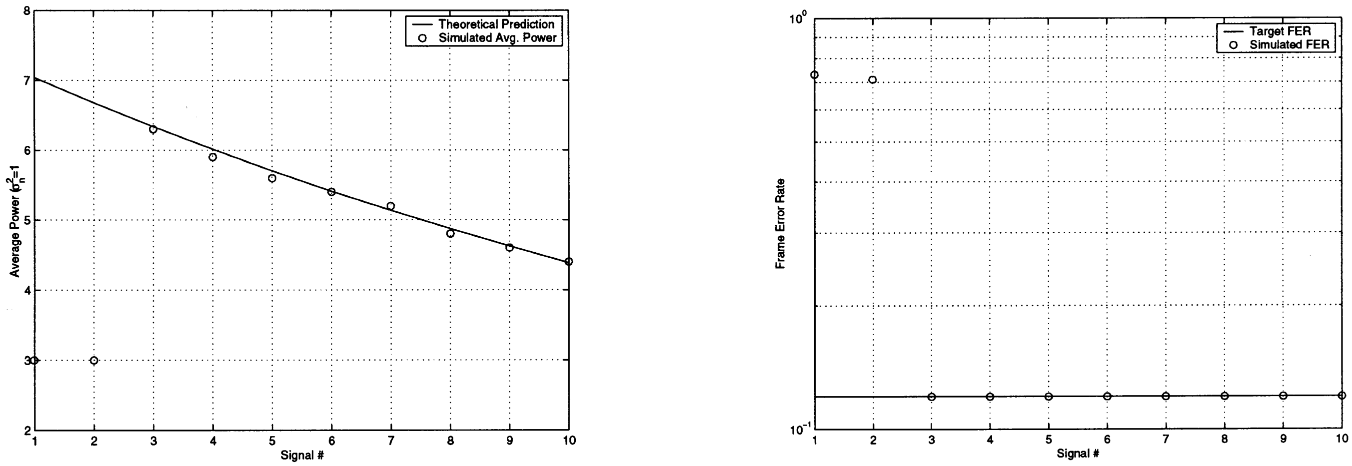

(a) (b)

Fig. 6. (a) Simulated and theoretical normalized ($\sigma_n^2 = 1$) received powers and (b) resulting FER for 12% target FER using FER-based outer-loop power control with SIC (perfect inner loop power control is assumed, $N = 64$, $K = 10$, signals 1 and 2 have received power limits of 3.0).

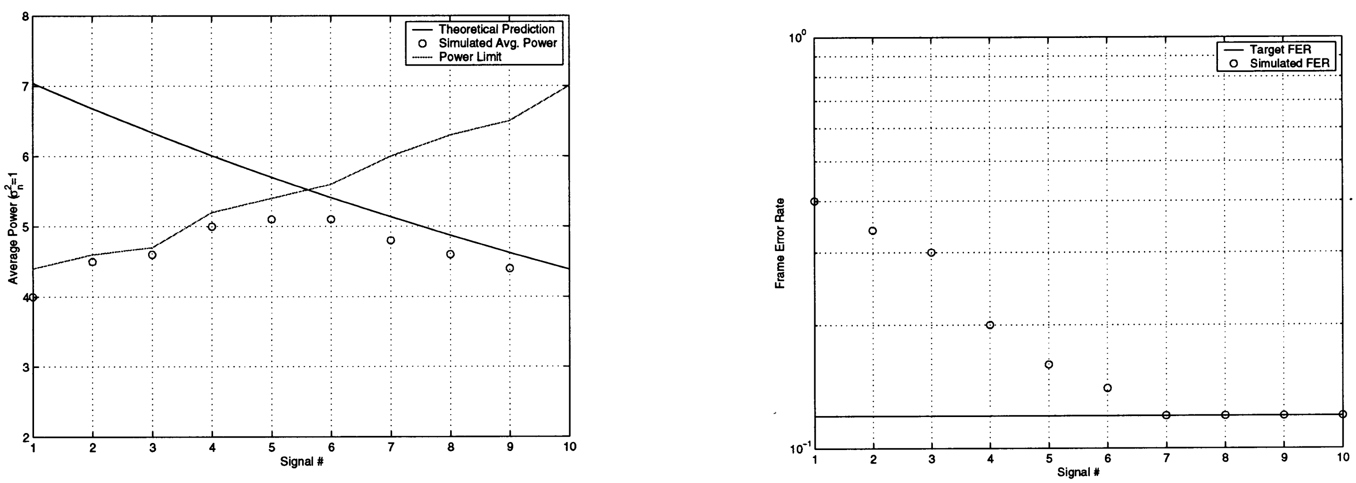

(a) (b)

Fig. 7. (a) Simulated and theoretical normalized ($\sigma_n^2 = 1$) received powers and (b) resulting FER for 12% target FER using FER-based outer-loop power control with SIC [perfect inner loop power control is assumed, $N = 64$, $K = 10$, all signals have received power limits shown in (a)].

the desired BER values. This would require power control tables for each cancellation slot and each number of total signals and SIR desired. However, as we will show, a better approach would be to use a generic set of values as a starting point and let the outer loop control the set points. Provided that all mobiles have sufficient power and the power vector is feasible, the outer loop will guarantee equal FER (or that all signals obtain their target FER values). Thus, the most obvious strategy is to assign those signals which have larger fade margins[6] to the early cancellation slots and those with smaller fade margins to the later cancellation slots. Such a scheme would have the added benefit of producing lower out-of-cell interference as discussed in [9]. The initial received energy estimate need not be perfect, just accurate enough to provide a reasonable ordering and can be obtained similar to open-loop power control at call setup. Specifically, during the initial acquisition process the searcher typically reports measured energy levels for finger assignment. This information could also be used for cancellation ordering. Alternatively, mobile based measurements used for hand-off processing could also be used for ordering purposes. The FER-based outer loop would then drive the set point to obtain the desired profile as we will show. The inner loop can use standard energy or E_b/I_o measurements along with the current set point to combat fading. Note that provided the E_b/I_o measurements are performed after cancellation, they will result in estimates that are consistent with the specific cancellation slot.

[6]Fade margin is inversely related to the total path loss and shadow fading experienced by the mobile.

IV. Convergence

It is of interest to examine the convergence of a BER-based power control algorithm. The convergence of general power control algorithms was discussed in [18]. Based on this work, it was shown in [19] that the deterministic BER-based algorithm

$$P_i(n+1) = \frac{\eta_i}{\ln\left\{\frac{1}{2\mathrm{BER}_i(\mathbf{p}(n))}\right\}} P_i(n) \tag{13}$$

where $\eta_i = \ln\{1/(2B_i)\}$ and B_i is the target error rate for user i, converges for a conventional matched filter receiver. We wish to show that (13) also converges to a fixed point for SIC receivers. Following [18], [19] the power control algorithm $\mathbf{p}(n+1) = \mathbf{T}(\mathbf{p}(n))$ converges to a fixed point provided that $\mathbf{T}(\mathbf{p})$ is a standard interference function. That is,

- the algorithm is positive: $\mathbf{T}(\mathbf{p}) > \mathbf{0}$ where $\mathbf{0}$ is the zero vector;
- the algorithm is monotonic: If $\mathbf{p} \geq \mathbf{p}'$ then $\mathbf{T}(\mathbf{p}) \geq \mathbf{T}(\mathbf{p}')$;
- the algorithm is scalable: For all $\alpha > 1, \alpha\mathbf{T}(\mathbf{p}) > \mathbf{T}(\alpha\mathbf{p})$.

In our case $\mathbf{T}_i(\mathbf{p}) = (\eta_i / \ln\{1/(2\mathrm{BER}_i(\mathbf{p}(n)))\})P_i(n)$ where $\mathrm{BER}_i(\mathbf{p}) = Q(\sqrt{\Gamma(\mathbf{p})})$, $\Gamma(\mathbf{p})$ is defined from (8) as $\Gamma(\mathbf{p}) = \mathbf{p^T Y^{-1}}$, $\mathbf{Y} = \mathrm{diag}\{\boldsymbol{\beta}\sigma^2 + (\varrho/N)\mathbf{Xp}\}$. We will now examine each condition in turn.

A. Positivity

To show that $\mathbf{T}(\mathbf{p}) > \mathbf{0}$, from the definition of $\mathbf{T}(\mathbf{p})$ we can see that we must show that $\ln\{1/(2Q(\sqrt{2\Gamma(\mathbf{p})}))\} > 0$. This is true provided that $Q(\sqrt{2\Gamma(\mathbf{p})}) < (1/2)$ which in turn is true provided that $\mathbf{p} > \mathbf{0}$ and $\sigma_n^2 < \infty$.

B. Scalability

To prove the scalability of $\mathbf{T}(\mathbf{p})$ we must show that $\alpha\mathbf{T}(\mathbf{p}) > \mathbf{T}(\alpha\mathbf{p})$ for $\alpha > 1$. That is, (14), as shown at the bottom of the page, where $\nu = (1 + (\varrho/N))$. Examining the denominators, we can rewrite our requirement as (15), shown at the bottom of the page, where the last requirement is true since $\alpha > 1$.

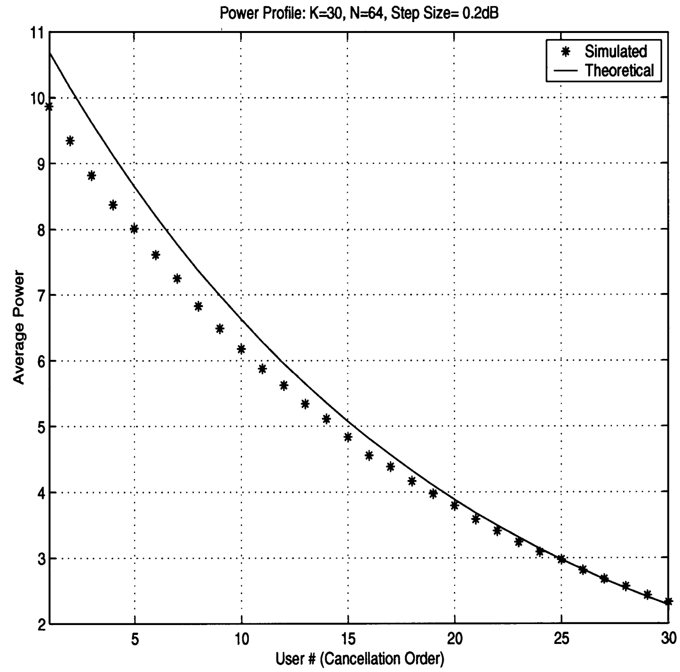

Fig. 8. Simulated and theoretical received powers for 12% target FER using FER-based outer-loop power control with SIC (synchronous, $N = 64$, $K = 30$, 0.2-dB step size, perfect inner loop power control assumed).

C. Monotonicity

To show that (13) is monotonic we must show that

$$\frac{\partial T_i\left(\mathbf{p}(n)\right)}{\partial P_j(n)} \geq 0 \qquad \forall i, j. \tag{16}$$

$$\begin{gathered}
\frac{\alpha\eta_i P_i}{\ln\left\{\frac{1}{2Q\left(\sqrt{2\Gamma_i(\mathbf{p})}\right)}\right\}} > \frac{\alpha\eta_i P_i}{\ln\left\{\frac{1}{2Q\left(\sqrt{2\Gamma_i(\alpha\mathbf{p})}\right)}\right\}} \\
\ln\left\{\frac{1}{2Q\left(\sqrt{2\Gamma_i(\mathbf{p})}\right)}\right\} < \ln\left\{\frac{1}{2Q\left(\sqrt{2\Gamma_i(\alpha\mathbf{p})}\right)}\right\} \\
Q\left(\sqrt{2\Gamma_i(\mathbf{p})}\right) > Q\left(\sqrt{2\Gamma_i(\alpha\mathbf{p})}\right) \\
\Gamma_i(\mathbf{p}) < \Gamma_i(\alpha\mathbf{p}) \\
\frac{P_i}{\left\{\left[\sigma_n^2 + \frac{\varrho}{N}\sum_{k=2}^K P_k\right]\nu^{i-1} - \frac{\varrho}{N}\sum_{k=2}^i \nu^{i-k}P_k\right\}} < \frac{\alpha P_i}{\left\{\left[\sigma_n^2 + \frac{\varrho}{N}\sum_{k=2}^K \alpha P_k\right]\nu^{i-1} - \frac{\varrho}{N}\sum_{k=2}^i \nu^{i-k}\alpha P_k\right\}}
\end{gathered} \tag{14}$$

$$\begin{gathered}
\left\{\left[\sigma_n^2 + \frac{\varrho}{N}\sum_{k=2}^K P_k\right]\nu^{i-1} - \frac{\varrho}{N}\sum_{k=2}^i \nu^{i-k}P_k\right\} > \left\{\left[\frac{\sigma_n^2}{\alpha} + \frac{\varrho}{N}\sum_{k=2}^K P_k\right]\nu^{i-1} - \frac{\varrho}{N}\sum_{k-2}^i \nu^{i-k}P_k\right\} \\
\sigma_n^2 + \frac{\varrho}{N}\sum_{k=2}^K P_k > \frac{\sigma_n^2}{\alpha} + \frac{\varrho}{N}\sum_{k=2}^K P_k \\
\frac{1}{\alpha} < 1
\end{gathered} \tag{15}$$

Now, to show that this is true for $j \neq i$ is straightforward. Increasing P_j will clearly degrade $\Gamma_i(\mathbf{p})$ for $j \neq i$ which will raise $Q(\sqrt{2\Gamma_i(\mathbf{p})})$ and thus increase P_i. Thus, we concentrate on showing that $\mathbf{T}(\mathbf{p})$ is monotonic for $i = j$. Accordingly, we arrive at (17), shown at the bottom of the page, where

$$I_i(\mathbf{p}) = \left\{ \left[\sigma_n^2 + \frac{\varrho}{N} \sum_{k=2}^{K} P_k \right] \left(1 + \frac{\varrho}{N}\right)^{i-1} - \frac{\varrho}{N} \sum_{k=2}^{i} \left(1 + \frac{\varrho}{N}\right)^{i-k} P_k \right\}. \quad (18)$$

$\Gamma_i(\mathbf{p})$ is defined by (19), shown at the bottom of the page, and $\delta_i = (\varrho/N)\{(1 + (\varrho/N))^{i-1} - 1\}$.

Now, simplifying (17)

$$\frac{\partial T_i(\mathbf{p})}{\partial P_i} = \frac{\eta_i}{\ln\left\{\frac{1}{2Q\left(\sqrt{\Gamma_i(\mathbf{p})}\right)}\right\}} \times \left\{ 1 - \frac{1}{2\sqrt{\pi}} \frac{\sqrt{\Gamma_i(\mathbf{p})}}{\ln\left\{\frac{1}{2Q\left(\sqrt{\Gamma_i(\mathbf{p})}\right)}\right\}} \frac{e^{-\Gamma_i(\mathbf{p})}\left[1 - \nu_i \Gamma(\mathbf{p})\right]}{Q\left(\sqrt{\Gamma_i(\mathbf{p})}\right)} \right\}. \quad (20)$$

Now, since $\delta_i \Gamma_i(\mathbf{p}) > 0$, we simply need to show that

$$\frac{\sqrt{x} e^{-x}}{2\sqrt{\pi} Q(\sqrt{2x}) \ln\left\{\frac{1}{2Q(\sqrt{2x})}\right\}} < 1 \quad (21)$$

for $0 < x < \infty$. In Fig. 2 we plot the above equation for $0 < x < 500$ and it can be seen that the inequality holds. Now, for larger x we simply examine the limit as $x \to \infty$. To do this we use the inequalities

$$Q(x) < \frac{1}{x\sqrt{2\pi}} e^{-\frac{x^2}{2}} \quad (22)$$

and

$$Q(x) > \frac{1}{x\sqrt{2\pi}} \left(1 - \frac{1}{x^2}\right) e^{-\frac{x^2}{2}} \quad (23)$$

to obtain

$$\frac{\sqrt{x} e^{-x}}{2\sqrt{\pi} Q(\sqrt{2x}) \ln\left\{\frac{1}{2Q(\sqrt{2x})}\right\}} < \frac{1}{\left(1 - \frac{1}{2x}\right)} \frac{1}{\frac{1}{2x}\ln\{\pi x\} + 1}. \quad (24)$$

Further

$$\lim_{x \to \infty} \frac{1}{\left(1 - \frac{1}{2x}\right)} \frac{1}{\frac{1}{2x}\ln\{\pi x\} + 1} = 1. \quad (25)$$

Thus, we conclude that $(\partial T_i(\mathbf{p})/\partial P_i)$ is positive, the power control relation $T(\mathbf{p})$ is indeed monotonic, and the power control algorithm $T(\mathbf{p})$ converges.

V. Stochastic Algorithm

The previous section showed that the deterministic power control algorithm based on BER (or equivalently FER) for SIC will converge. However, the algorithm described in Section II is a stochastic version of an FER-based power control algorithm. Specifically, if $q_i(n) = 10\log_{10} P_i(n)$, we can write the standard (outer loop) power control algorithm in decibels as

$$q_i(n+1) = q_i(n) + \Delta\left\{\hat{f}_i - \frac{\eta_i}{1 - \eta_i}(1 - \hat{f}_i)\right\} \quad (26)$$

where η_i is the target error rate for user i, $\hat{f}$ is the estimated FER and Δ is the algorithm step size. The FER estimate is typically a one bit estimate based on a CRC

$$\hat{f}_i = \begin{cases} 1, & \text{CRC check fails} \\ 0, & \text{CRC check passes.} \end{cases} \quad (27)$$

$$\begin{aligned} \frac{\partial T_i(\mathbf{p})}{\partial P_i} &= \frac{\ln\left\{\frac{1}{2Q\left(\sqrt{2\Gamma_i(\mathbf{p})}\right)}\right\} \frac{\partial(\eta_i P_i)}{\partial P_i} - \eta_i P_i \frac{\partial}{\partial P_i}\left\{\ln\left\{\frac{1}{2Q\left(\sqrt{2\Gamma_i(\mathbf{p})}\right)}\right\}\right\}}{\left\{\ln\left\{\frac{1}{2Q\left(\sqrt{2\Gamma_i(\mathbf{p})}\right)}\right\}\right\}^2} \\ &= \frac{\ln\left\{\frac{1}{2Q\left(\sqrt{2\Gamma_i(\mathbf{p})}\right)}\right\} \eta_i - \eta_i P_i \cdot 2Q\left(\sqrt{2\Gamma_i(\mathbf{p})}\right) \frac{\partial}{\partial P_i}\left\{\frac{1}{2Q\left(\sqrt{2\Gamma_i(\mathbf{p})}\right)}\right\}}{\left\{\ln\left\{\frac{1}{2Q\left(\sqrt{2\Gamma_i(\mathbf{p})}\right)}\right\}\right\}^2} \\ &= \frac{\ln\left\{\frac{1}{2Q\left(\sqrt{2\Gamma_i(\mathbf{p})}\right)}\right\} \eta_i - \eta_i P_i \cdot 2Q\left(\sqrt{2\Gamma_i(\mathbf{p})}\right) \frac{1}{2Q\left(\sqrt{2\Gamma_i(\mathbf{p})}\right)} \frac{e^{-\Gamma_i(\mathbf{p})}}{\sqrt{4\pi\Gamma_i(\mathbf{p})}} \frac{1 - \Gamma_i(\mathbf{p})\delta_i}{I_i(\mathbf{p})}}{\left\{\ln\left\{\frac{1}{2Q\left(\sqrt{2\Gamma_i(\mathbf{p})}\right)}\right\}\right\}^2} \end{aligned} \quad (17)$$

$$\Gamma_i(\mathbf{p}) = \frac{P_i}{\left\{\left[\sigma_n^2 + \frac{\varrho}{N}\sum_{k=2}^{K} P_k\right]\left(1 + \frac{\varrho}{N}\right)^{i-1} - \frac{\varrho}{N}\sum_{k=2}^{i}\left(1 + \frac{\varrho}{N}\right)^{i-k} P_k\right\}} \quad (19)$$

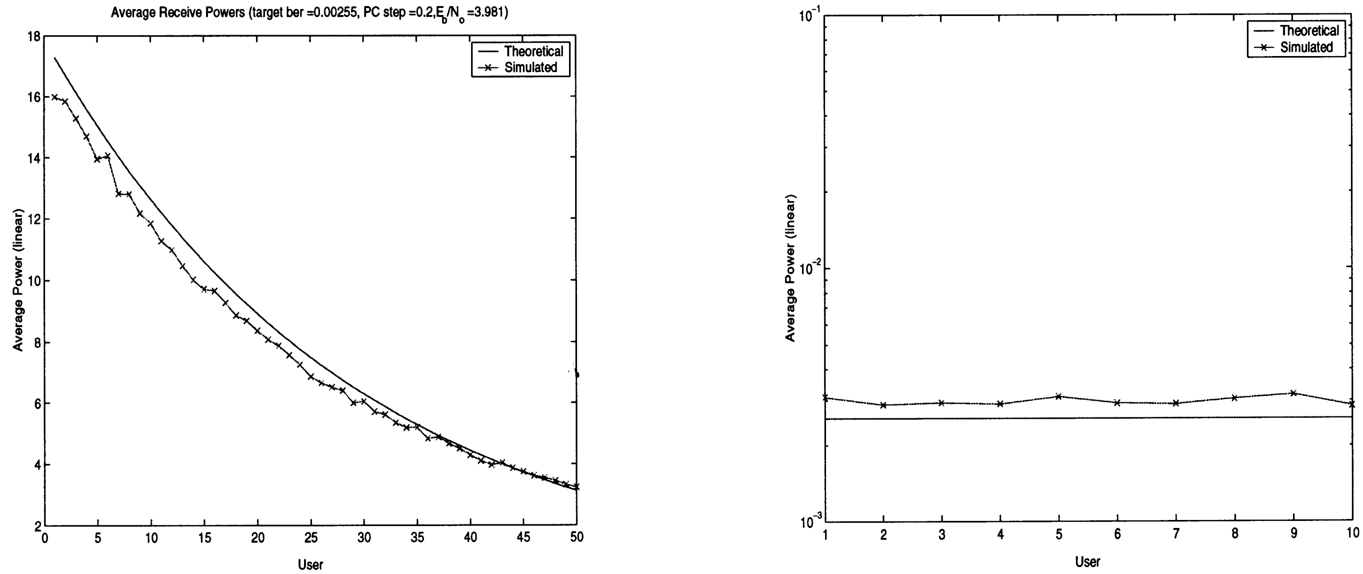

Fig. 9. Simulated and theoretical average power profile and FERs using FER-based outer-loop power control with SIC (perfect inner loop power control is assumed, asynchronous, $N = 64$, random phases, $K = 50$, 0.2-dB step size).

Specifically, this algorithm corresponds to the power control iteration

$$P_i(n+1) = P_i(n)10^{0.1\Delta\left[f_i - \frac{\eta_i}{1-\eta_i}(1-f_i)\right]} \tag{28}$$

which can be shown to converge in a manner similar to the previous section. The algorithm in (26) can also be implemented in terms of BER by using training bits as

$$q_i(n+1) = q_i(n) - \frac{1}{2}\frac{y\Delta}{100-y}\left[\text{sgn}\left\{b_i(n)z_i(n)\right\}+1\right] + \frac{1}{2}\Delta\left[1-\text{sgn}\left\{b_i(n)z_i(n)\right\}\right] \tag{29}$$

where $\hat{B}_i = (1/2)\{1 - \text{sgn}\{b_i(n)z_i(n)\}\}$ is the instantaneous BER estimate. We can easily show that $\hat{B}_i$ is an unbiased estimate of the true BER (B_i). That is,

$$\lim_{M\to\infty}\frac{1}{M}\sum_{i=1}^{M}\hat{B}_i = B_i. \tag{30}$$

Thus, on average the power control iteration will have the correct update. A detailed analysis of the convergence of the stochastic algorithm is currently being investigated.

VI. Results

Simulations were run using the SIC receiver along with the stochastic FER-based outer-loop power control as described above. It was assumed that inner loop power control was perfect and that the system was synchronous with random phases and random spreading codes. The powers were all started at unity (i.e., $P_i(0) = 1$). The outer loop used a step size of $\Delta = 0.3$ dB per frame error. Coding was not used and frame errors were defined as the event where any one or more of the bits in the frame was in error. The frame size considered was 50 bits. Since coding was not used the target FER considered was fairly high at 12% which corresponds to approximately a 0.2% BER. These simulations assumed a spreading gain of $N = 64$ and $K = 10$ signals. It can be shown that this BER requires an SINR of 6 dB.

Fig. 3 presents the average received power for each of the ten signals in the system when no power limits are placed on the mobiles. The predicted normalized power from (10) with an SINR $\Gamma = 6$ dB is also plotted with $\sigma_n^2 = 1$. Note that signals are ordered according to decreasing received power which is also the cancellation order. All signals obtained the target 12% frame error rate. Thus, the outer loop converged (on average) to the optimal power vector given in (10). Note, that after convergence, the stochastic algorithm will move the instantaneous power vector around the optimal power vector based on the occurrence of frame errors and the step size as shown in (26). The smaller the step size, the smaller the variation but the longer the convergence time. The main assumption here is that all mobiles have sufficient power for the cancellation slot they are assigned. However, this requires intelligent assignment of cancellation order. If the first signal in the cancellation order corresponds to the signal furthest from the base station, not only will it result in more out-of-cell interference [9], but it is possible that the signal will have insufficient power to achieve its target. A coarse knowledge is available from open-loop power control at call setup or via hand-off measurements as mentioned.

To determine the effect that such a limit (i.e., incorrect cancellation order) would have on the receiver performance we examined the performance of the stochastic algorithm in cases where some mobiles have a power limit. In the first example shown in Fig. 4, signal 4 is limited to a normalized received power (i.e., $\sigma_n^2 = 1$) of 4.4 (i.e., SNR $= 4.4$). As we can see from Fig. 4, this prevents signal 4 from achieving its target FER since the power limit is below that necessary for the assigned cancellation slot. If that signal were assigned to the first cancellation slot, it would have achieved the target FER. Of further interest is the effect that the power-limited signal has on those signals which are cancelled before and after it. Signals cancelled before the power-limited signal (#1–3) benefit in that they see less

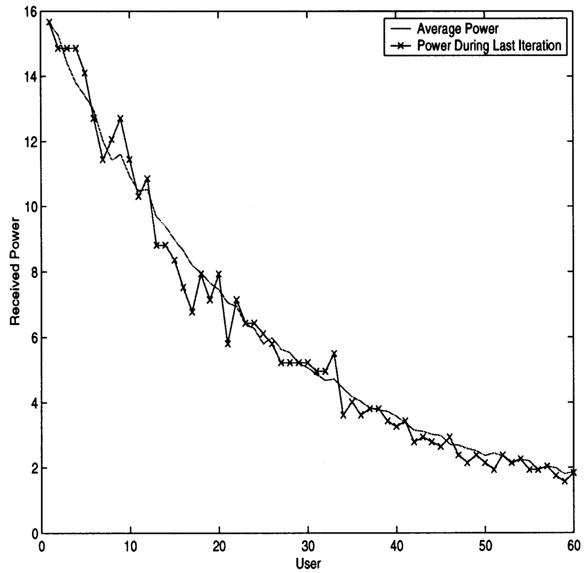

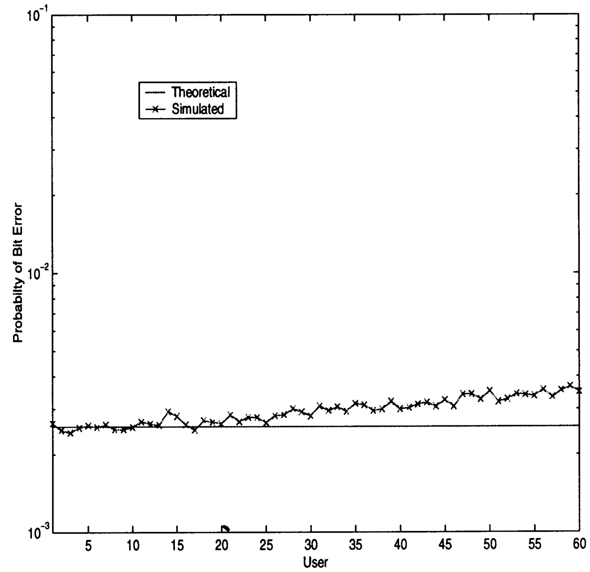

Fig. 10. Simulated and theoretical average power profile and FERs using FER-based outer-loop power control with nonlinear SIC (perfect inner-loop power control is assumed, asynchronous, $N = 64$, random phases, $K = 60$).

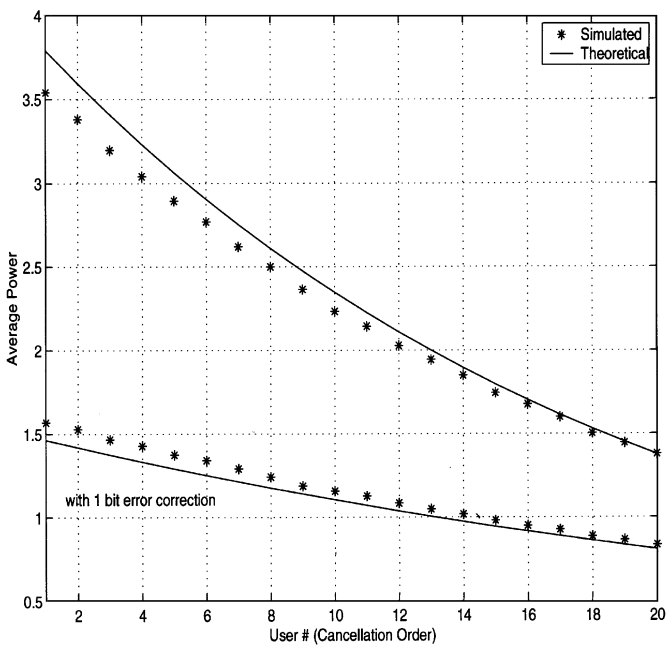

Fig. 11. Simulated and theoretical received powers for 12% target FER using FER-based outer-loop power control with SIC with and without coding (synchronous, $K = 20$, $N = 64$, 0.2-dB step size, perfect inner loop power control assumed).

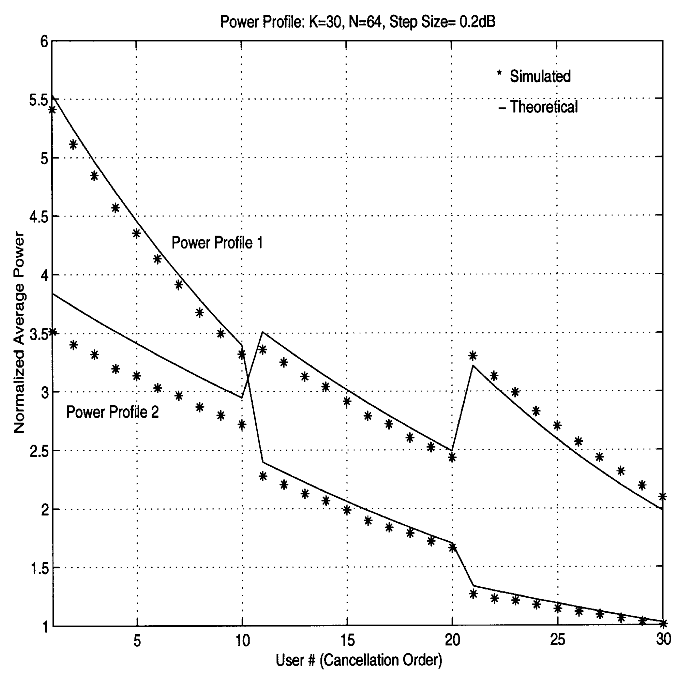

Fig. 12. Simulated and theoretical received powers for two quality of service profiles using FER-based outer-loop power control with SIC with two different cancellation orders (synchronous, $K = 30$, 0.2-dB step size, perfect inner loop power control assumed, 0.2%, 0.7%, and 1.4% BER targets).

interference power (due to the lower received power of signal 4) and thus can transmit less power and still achieve the target FER. Signals which are cancelled after the power-limited signal are nearly unaffected by the increased error rate and the lower received power. The effect of higher error rate (which increases interference) is offset by the lower received power (which decreases interference).

In Fig. 5 signals 9 and 10 are limited to a normalized value of 3. These signals cannot reach the FER target but the others signals are not affected in terms of performance. Since these are the last two signals cancelled, the limits have the effect of reducing the necessary transmit power required for the signals cancelled before them.

A more serious potential problem is a limit on the first two signals cancelled as shown in Fig. 6. Here it is anticipated that since the first two signals will not achieve their target FER, they will not be cancelled properly and will thus introduce more interference to those signals cancelled afterwards due to error propagation. However, since they are power limited, their effect is both increased (due to inaccurate cancellation) and decreased (due to reduced power). The net effect is that the signals cancelled afterward require essentially the same receive power as

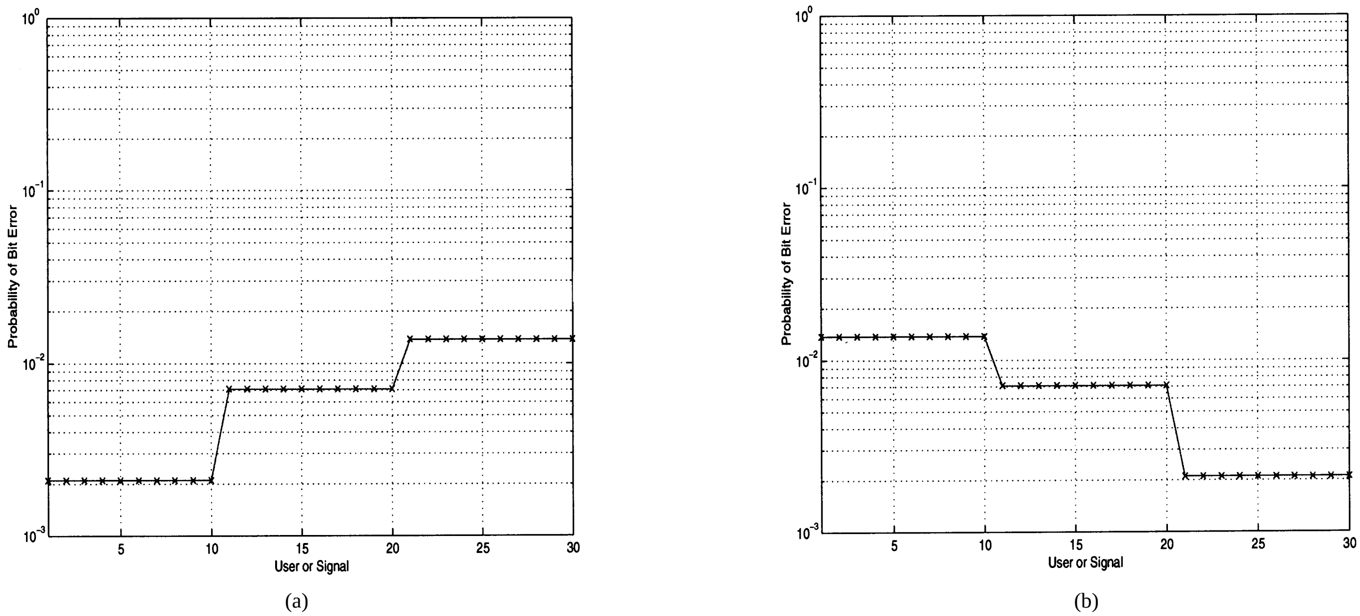

Fig. 13. Simulated BERs using FER-based outer-loop power control with SIC (perfect inner loop power control is assumed, signals achieved power profiles shown in Fig. 12).

without the limits. The receiver with SIC and power control is thus fairly robust. The main problem then with inaccurate ordering is: 1) the performance of the mobile in question may be degraded (i.e., it may not achieve target) and 2) the system creates larger out-of-cell interference than with proper ordering.

As a last example of power limitations, Fig. 7 plots the average received power and the achieved frame error rate for the power limits shown in Fig. 7(a). This essentially represents an ordering which is the opposite of the optimal ordering scheme since the more limited signals are cancelled first and the less limited signals are cancelled last. Again, we see that signals which are power-limited cannot reach their target FER, but they do not have an adverse effect on the other signals in the system. Again, this suggests that the SIC receiver with outer-loop power control is fairly robust. The base station need not specify separate fine-tuned threshold tables for each cancellation situation in order for SIC to be effective. Instead, the base station simply needs to have a rough idea of the relative shadow fading and path loss (as a gauge to the relative power limits of the mobiles) in order to make an ordering assignment. This can be gauged by using energy estimates obtained by the searcher and acquisition circuitry or from handoff measurements. Further, FER is estimated at the base station. If a particular signal is not meeting its FER target, it can be moved down in the cancellation order to improve its performance based on its power limit. This order control can be done at a much slower rate to combat long term fading changes. System software can detect high FER values and instruct the base station to move the signal down in the cancellation order.

The previous examples have examined fairly light loading levels. Fig. 8 presents the average received power levels and BERs for a higher loading level of 30 users with $N = 64$ and synchronous reception and random codes. The algorithm used a step size of $\Delta_p = 0.2$ dB, the same target FER (12%), 50 bit frames (corresponding to a target BER of 0.2%) and no power limits. The predicted power profile matches well with the predicted profile and the target error rate is achieved. As a further test in higher loading conditions, Fig. 9 presents results for the asynchronous case with $K = 50$ users and all other parameters being the same as in the previous case. Again, the theoretical power profile and target error rates match well with the simulated values although we do see a slight rise in the average FER due to a longer convergence time. As a final loading test, we examine the performance of nonlinear SIC (i.e., with hard decisions and perfect channel estimation). In Fig. 10 we plot the achieved power profile and error rates for the case of $K = 60$ users, $N = 64$, a 0.2-dB step size, and a 12% target FER. Since the theoretical profile derived previously is for linear SIC, it cannot be applied to the nonlinear case. Thus, we plot the average power profile along with the powers during the last iteration. The plot shows that the final power values are very close to the average meaning that the algorithm has likely converged. This is also seen in the fact that the error rate is very close to the target error rate. There is some deviation for the signals late in the cancellation order as can be seen. This could be due to the fact that the case is a particularly stressing one (loading nearly equal the spreading gain) which typically requires longer convergence time.

As noted previously, we have not assumed the use of any error correction coding. To briefly examine the impact of coding, we simply examine the case where a frame error is defined as the event where 2 or more bit errors occur in a frame (i.e., one error per frame correction). This results in a higher tolerated BER and thus lower required power levels as shown in Fig. 11. The simulation examines the synchronous case with 20 users, $N = 64$, a 0.2-dB step size, and a target FER of 12%. The power profiles are plotted for the cases of no error correction coding and one error per frame correction. The algorithm maintained the target frame error rate of 12% in both cases. The profiles show the expected result that the coded case requires a significantly lower received power profile corresponding to a higher BER.

Each of the previous examples assumed that the target error rate of each user was the same. As shown in (12) we can de-

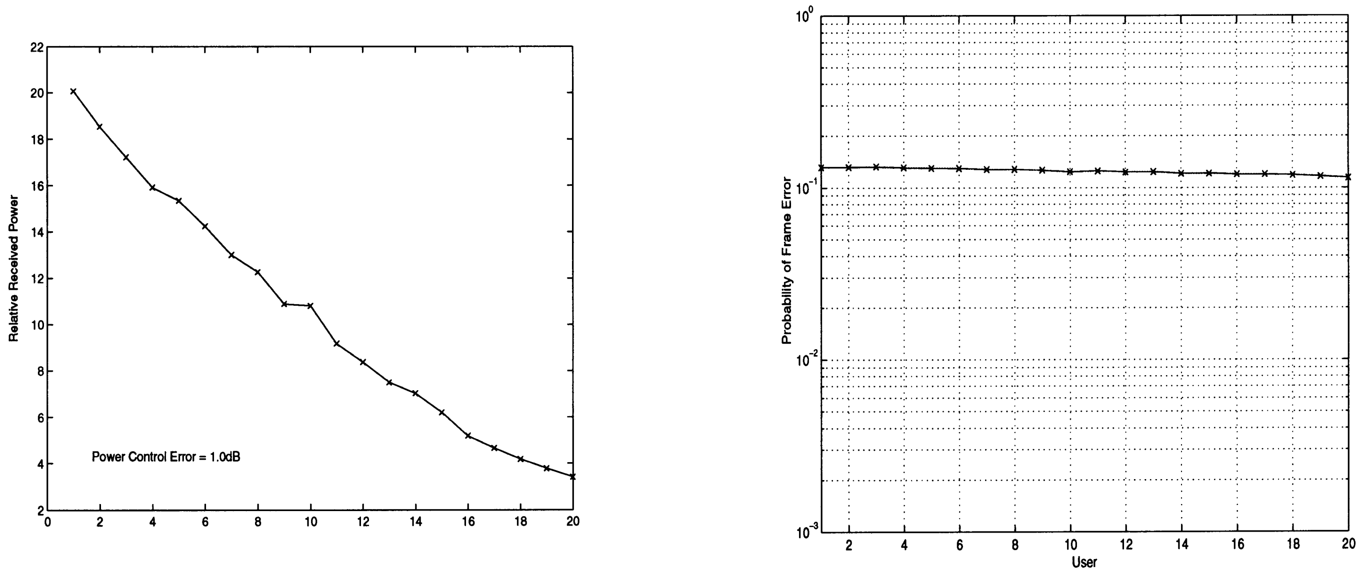

Fig. 14. Simulated average power profile and FER using FER-based outer-loop power control with SIC (power control error $\sigma = 1$ dB, synchronous, $N = 64$, random phases, $K = 20$, 0.2–dB step size).

rive the power profile for various target error rates (sometimes called different qualities of service). The power profiles and average error rates for BER targets of 0.2%, 0.7%, and 1.4%, with 30 users (ten users per target BER), $N = 64$, a 0.2-dB step size and synchronous reception were obtained and plotted in Figs. 12 and 13. Note that we examined two different orderings as shown in Figs. 12 and 13 and that the simulated values match well with the theoretical predictions. The error rates in 13(a) correspond to power profile 1 in Fig. 12, and 13(b) corresponds to power profile 2. In the multiple target case, ordering must also consider the groups of users, since different targets correspond to different profiles. We can see that by cancelling the signals with higher FER targets, we obtain in lower maximum power requirements and smaller disparities between received powers. On the other hand, if we cancel signals with lower FER targets first, we require a more accentuated profile.

Finally, we briefly examine the impact of inner loop power control error. While the convergence analysis done in Section IV assumed perfect inner loop power control, we postulate that provided the K-fold distribution of the power vector $\mathbf{p}$ necessary to achieve the target error rates is feasible, the algorithm will converge. The only case examined in detail in this work considered a log-normal power control error with $\sigma = 1$ dB. The resulting power profile and achieved error rates are given in Fig. 14. The examined case is for $K = 20$ synchronous signals, a 0.2-dB step size, and a 12% target error rate. The average power profile is shown along with the achieved error rates. Again, the target was achieved with an exponential power profile, although significantly more power is needed than in the case of perfect inner-loop power control. A more detailed analysis of the impact of inner-loop power control error will be reserved for future work.

VII. Conclusion

In this paper, we have shown that FER-based outer-loop power control can be used with successive interference cancellation to provide stable error rate performance without having sophisticated power threshold tables. A deterministic BER-based (or equivalently, FER-based) power control algorithm was shown to converge for SIC and the performance of the stochastic algorithm was demonstrated in several simulations. Further, it was shown that the effect of making errors in the assignment of cancellation order does not have an adverse effect on the system as a whole. Rather, it affects only the signal which is limited. This effect can be detected at the base station by monitoring FER and making corrections in the cancellation order. We examined different loading factors, as well as the case of multiple target error rates. We also briefly examined the impact of coding and inner loop power control error. Future work should further investigate the impact of power control errors and convergence time, conduct a convergence analysis of the stochastic algorithm, and investigate algorithms for changing the cancellation order.

Acknowledgment

The first author of this paper wishes to acknowledge the support, assistance, guidance, and stimulating discussions provided by his colleagues at Lucent Technologies-Bell Labs. These include S. Nicoloso, R. Benning, R. Soni, D. Uptegrove, F. Dominique, and L. Mailaender. The authors would also like to thank the anonymous reviewers who greatly improved the quality of this paper through their comments.

References

[1] A. Duel-Hallen, J. Holtzman, and Z. Zvonar, "Multiuser detection for CDMA systems," *IEEE Pers. Commun.*, vol. 2, pp. 46–58, Apr. 1995.
[2] S. Moshavi, "Multi-user detection for DS-CDMA communications," *IEEE Commun. Mag.*, vol. 34, pp. 124–137, Oct. 1996.
[3] S. Verdú, *Multiuser Detection*. New York: Cambridge Univ. Press, 1998.
[4] A. Viterbi, "Very low rate convolutional codes for maximum theoretical performance of spread-spectrum multiple-access channels," *IEEE J. Select. Areas Commun.*, vol. 8, pp. 641–649, May 1990.

[5] P. Patel and J. Holtzman, "Analysis of a simple successive interference cancellation scheme in a DS-CDMA system," *IEEE J. Select. Areas Commun.*, vol. 12, pp. 796–807, June 1994.
[6] H. Fujii and S. Tachikawa, "Improvement methods of propagation error for multiple access interference successive cancellation techniques in DS-CDMA," *IEICE Trans. Fundam. Electron. Commun. Comput. Services*, vol. E81-A, pp. 1423–1429, July 1998.
[7] G. Mazzini, "Equal BER with successive interference cancellation DS-CDMA systems on AWGN and Ricean channels," in *Proc. 1995 Personal, Indoor, and Mobile Radio Conf.*, July 1995, pp. 727–731.
[8] K. Pedersen, T. Kolding, I. Seskar, and J. Holtzman, "Practical implementation of successive interference cancellation in DS/CDMA systems," in *Proc. 1996 Universal Personal Communications Conf.*, 1996.
[9] P. Hatrack and J. Holtzman, "Reduction of other-cell interference with integrated interference cancellation/power control," in *Proc. Vehicular Technology Conf.*, 1997, pp. 1842–1846.
[10] R. M. Buehrer, "Equal BER performance in linear successive interference cancellation," *IEEE Trans. Commun.*, vol. 49, pp. 1250–1258, July 2001.
[11] P. Kumar and J. Holtzman, "Power control for a spread spectrum system with multiuser receivers," in *Proc. 1995 Personal, Indoor, and Mobile Radio Conf.*, July 1995, pp. 955–959.
[12] M. Varanasi, "Stochastic power control for nonlinear multiuser receivers in cellular radio networks," in *Proc. 1999 IEEE Information Theory Workshop*, Kruger National Park, South Africa, June 20–25, 1999, pp. 18–20.
[13] P. Viswanath, V. Anantharam, and D. Tse, "Optimal sequences, power control, and user capacity of synchronous CDMA systems with linear MMSE multiuser receivers," *IEEE Trans. Inform. Theory*, vol. 45, pp. 1968–1983, Sept. 1999.
[14] A. Yener, R. Yates, and S. Ulukus, "Joint power control, multiuser detection and beamforming for CDMA systems," in *Proc. 49th Vehicular Technology Conf.*, Houston, TX, May 16–20, 1999.
[15] A. Almutairi, S. Miller, H. Latchman, and T. Wong, "Power control algorithm for MMSE receiver based CDMA systems," *IEEE Commun. Lett.*, vol. 4, pp. 346–348, Nov. 2000.
[16] M. Saquib, R. Yates, and A. Ganti, "Power control for an asynchronous multirate decorrelator," *IEEE Trans. Commun.*, vol. 48, pp. 804–812, May 2000.
[17] M. B. Pursley, "Performance evaluation for phase-coded spread-spectrum multiple-access communication—Part I: System analysis," *IEEE Trans. Commun.*, vol. COM-25, pp. 795–799, Aug. 1977.
[18] R. Yates, "A framework for uplink power control in cellular radio systems," *IEEE J. Select. Areas Commun.*, vol. 13, pp. 1341–1347, Sept. 1995.
[19] P. Kumar, R. Yates, and J. Holtzman, "Power control based on bit error rate measurements," in *Proc. 1995 Military Communications Conf.*, 1995, pp. 617–620.

R. Michael Buehrer (S'91–M'96) joined Virginia Polytechnic Institute and State University (Virginia Tech), Blacksburg, in 2001. He is currently an Assistant Professor in the Bradley Department of Electrical Engineering, where he works with the Mobile and Portable Radio Research Group. His current projects include propagation measurement and channel modeling of ultra-wideband signals as part of the DAPRA NETEX program. Other projects include MIMO system design, multiuser detection, spread spectrum, software radio research, communication system optimization, adaptive antennas, spatial channel modeling, adaptive modulation and coding, and OFDM-based modulation techniques. From 1996 to 2001, he was with Bell Laboratories—Lucent Technologies, working in the areas of CDMA receiver design, multiuser detection, adaptive antennas, and spatial channel modeling. He has coauthored more than a dozen journal and 25 conference papers and holds seven patents in the area of wireless communications.

Dr. Buehrer was named Outstanding New Assistant Professor by the Virginia Tech College of Engineering in 2003.

Rahul Mahajan (S'01) was born in Mumbai, India, in 1979. He received the Bachelor of Engineering degree in electronics and telecommunications from the University of Pune, Pune, India, in 2001. He is currently working toward the M.S. degree in electrical engineering at Virginia Polytechnic Institute and State University (Virginia Tech), Blacksburg.

He is a Research Assistant in the Mobile and Portable Radio Research Group at Virginia Tech, where his interests include cross-layer optimization, CDMA systems, radio resource management, and ad hoc networks.

Mr. Mahajan served as the Outreach Chair for the Virginia Tech IEEE Chapter from 2001 to 2002.